

High-efficiency blue-light generation by frequency doubling of picosecond pulses in a thick KNbO₃ crystal

Yong-qing Li

Department of Physics, East Carolina University, Greenville, North Carolina 27834-4353

Dorel Guzun, Greg Salamo, and Min Xiao

Department of Physics, University of Arkansas, Fayetteville, Arkansas 72701

Received August 5, 2002; revised manuscript received December 10, 2002

We report an experimental demonstration of highly efficient single-pass second-harmonic generation from 859 nm to 429.5 nm with picosecond pulses in a thick KNbO₃ crystal. Both the conversion-efficiency and quantum-noise properties of the generated blue pulses are measured at various pump intensities under a strong focusing condition. We find that the variation of the conversion efficiency of the picosecond second-harmonic generation is an oscillatory function of the input pump intensity (with a maximum efficiency of 56.5%) and is sensitive to the position of the input beam focus in the crystal. The quantum noise on the blue beam can be reduced below the shot-noise limit by 20% at low input power. © 2003 Optical Society of America
OCIS codes: 190.2620, 270.6570.

1. INTRODUCTION

Second-harmonic generation (SHG) is an attractive optical frequency conversion process to generate coherent light at shorter wavelengths.¹ Very high conversion efficiency has been reported under extremely high pump intensities,²⁻⁴ i.e., an efficiency of 92% from 1064 nm to 532 nm in bulk nonlinear crystals with a typical pump intensity of a few GW/cm².² Recently, single-pass traveling-wave (TW) SHG with cw mode-locked pulses has attracted attention because of low average input power with high peak intensity, and conversion efficiency higher than 60% has been obtained both in bulk nonlinear crystals⁵⁻⁸ (NLCs) and in quasi-phase-matched nonlinear waveguides.^{9,10} Highly efficient TW SHG at a low average input power is an interesting nonlinear optical system that not only conveniently provides a coherent light source at short wavelengths, but also allows generation and observation of amplitude-squeezed light that has less-intensity noise than the standard shot-noise limit.^{7,11} In fact, 6.7% (0.3-dB) amplitude squeezing in SHG was observed with a conversion efficiency of 15% in the TW SHG experiment with a type II phase-matched bulk KTP crystal.¹¹ In an experiment with a LiNbO₃ waveguide,⁹ 16.8% (0.8-dB) squeezing in the transmitted fundamental field and 7.7% (0.35 dB) squeezing in the generated harmonic light were observed with a conversion efficiency approaching 60%. In the TW SHG with a thick potassium niobate (KNbO₃) crystal pumped by femtosecond pulses, a slope efficiency of 300% nJ⁻¹ for harmonic conversion was achieved⁵ and a 20% (1.0-dB) squeezing in the generated harmonic light was observed with a conversion efficiency of 60% at ~90 mW average input power.^{7,12}

In this paper, we study highly efficient single-pass SHG

in a thick, noncritically phase-matched KNbO₃ crystal pumped by picosecond pulses and measure the quantum-noise properties of the generated blue pulses. We show that the TW SHG process in KNbO₃ with picosecond pulses is quite different from that with femtosecond pulses. Much less peak intensity is necessary to obtain the high conversion efficiency for picosecond pulses under the strong focusing condition. We found that the variation of the conversion efficiency of the picosecond SHG is an oscillatory function of the input pump intensity (with a maximum efficiency of 56.5%) and is sensitive to the position of the input beam focus in the crystal. The quantum noise on the blue beam can be reduced below the shot-noise limit by 20% at low input power.

2. BACKGROUND

KNbO₃ is an attractive nonlinear crystal that has a large nonlinear coefficient and noncritical phase matching (no spatial walk-off) under appropriate conditions for low-power optical applications.¹³⁻¹⁵ However, this crystal also has a large group-velocity mismatch ($\alpha = 1.2$ ps/mm for the wavelength conversion from 860 nm to 430 nm) and a narrow phase-matching bandwidth of $\Delta\nu = 0.88/\alpha L$ (~ 0.2 nm for a crystal length of $L = 10$ mm),⁶ which generally limit it from short-pulse, wideband applications. In the previous TW SHG experiments with femtosecond pulses,⁵⁻⁸ the input spectral width (~ 10 nm for a Gaussian pulse with duration time $t_p = 120$ fs) is much broader than the phase-matching bandwidth. Thus the temporal walk-off length $l_T = t_p/\alpha$ (~ 100 μ m), over which a fundamental pulse and a harmonic pulse miss temporal overlap from each other completely, is much

shorter than the crystal length L (3–10 mm). Therefore the femtosecond SHG in a long crystal can be considered as a series of independent SHG processes in each thickness of l_T of the crystal due to the group-velocity mismatching, similar to the SHG in a quasi-phase-matched material. Assuming noncritical phase matching, low pump depletion, and $l_T < b$ in each length of l_T , the total conversion efficiency is then given by $\eta_{\text{tot}} = \eta_1(L/l_T)$, where $\eta_1 = \gamma P_\omega(l_T^2/b)$ is the conversion efficiency in each length l_T , P_ω is the peak power of the fundamental frequency, $b = (2\pi w_0^2 n)/\lambda$ is the depth of the focus, w_0 is the beam radius at the focus, n is the index of refraction of the crystal, and γ is a constant describing the nonlinear coefficient of the crystal.⁶ Under this condition, the generated blue pulse is much longer (typically picosecond) than the input fundamental pulses. The broadband femtosecond input pulses are upconverted to generate narrow-band blue pulses. Because the walk-off length l_T is very short, the conversion efficiency η_1 in the thickness of l_T is very low ($\eta_1 \ll 1$) even with high peak power of the input pulses, and therefore the pump depletion in each l_T can be neglected. The observed squeezing ($\sim 20\%$) in the generated blue pulses is considered as being limited by the effective length of nonlinear interaction between the infrared and blue pulses of the order of η_1 .⁷

In current picosecond SHG, the temporal walk-off length l_T (~ 1.7 mm for $t_p = 2.0$ ps) is much longer than that in the femtosecond case such that the phase-matching nonlinear interaction length in the crystal is significantly increased. Under the strong focusing condition ($b < L$), the effective interaction length in the crystal becomes approximately b (~ 1.83 mm for a $f = 50$ mm lens) such that $l_T \approx b < L$. Therefore approximately only one thickness of l_T of the crystal contributes to the blue-light generation so that $\eta_{\text{tot}} \sim \eta_1$, and the efficiency η_1 can be very high ($\sim 50\%$) in the picosecond case. In this case, pump depletion in l_T is significant. Also, the spectral bandwidth (~ 0.6 nm) of the fundamental picosecond pulses is less than or comparable to the phase-matching bandwidth (~ 1.0 nm for an effective length b of 1.83 mm) so that almost all the spectral components in the fundamental pulses efficiently upconvert to the harmonic pulses in the frequency-doubling process. These advantages over the femtosecond pump make the picosecond SHG in KNbO₃ crystal more efficient, which means that a lower peak power (compared with the femtosecond case) is adequate to obtain the same SHG conversion efficiency. In our experiment, we have demonstrated that the peak power for picosecond pulses was reduced by a factor of ~ 20 compared with that for femtosecond pulses to achieve the same conversion efficiency. Since the conversion efficiency η_1 in the thickness of l_T is high, one might expect to generate a larger amount of squeezing in the generated blue pulses, as in the case of cw SHG.¹⁵ However, both the pump depletion in l_T and phase modulation may affect the total conversion efficiency and reduce the achievable quantum-noise reduction in the blue pulses. To the best of our knowledge, high-efficiency TW SHG pumped by picosecond pulses in the strong focusing condition ($l_T \approx b < L$) and quantum-noise properties in a thick NLC have not been studied experimentally.

3. EXPERIMENTAL SETUP

A mode-locked Ti:sapphire laser generating ~ 2.0 -ps pulses with 80-MHz repetition rate at 859 nm was used in our experiment. The fundamental beam was focused onto an a -cut, 10-mm-thick KNbO₃ crystal with a lens of 5-cm focal length. The strong focusing condition ($b < L$) is satisfied with this focal length. The entrance surface of the KNbO₃ crystal is antireflection coated for 860 nm, and the exit surface is antireflection coated for 430 nm. The crystal was kept at a temperature of 25.5 °C with a precision temperature controller to achieve the noncritical phase-matching condition. The wavelength of the Ti:sapphire oscillator was tuned to 859.4 nm to obtain optimum phase matching, and the input average power was variable from 0 to 500 mW with a pair of polarizers. The crystal was mounted on a translation stage, and the position of the crystal center can be moved relative to the focal point of the input beam. The output blue light was collected with a 5-cm lens, filtered with an IR filter, and then detected with a digitized powermeter for average power. The overall conversion efficiency was calculated from the ratio of the synchronously recorded output blue power and the input IR power.

The quantum noise of the generated blue light was measured with a balanced homodyne detection system,^{7,12} composed of a 50–50 beam splitter and two identical photodiodes (Hamamatsu S3994). The photodiodes are placed at an angle to the incident blue light beam, and the reflected blue light from the photodiode's front surface is reflected back to the photodiode by a mirror closely placed next to each photodiode. With this arrangement, the quantum efficiency of the photodiodes at 428.8 nm is increased. The overall detection efficiency for the blue light from the exit surface of the crystal to the output photocurrents of the photodiodes is estimated to be 0.70. The output photocurrent from each photodiode is first coupled to a low-pass filter (DC–32 MHz) to remove the 80-MHz signal of the laser mode-locking frequency and then ac-coupled to a low-noise preamplifier. The low-pass filters effectively avoid saturation of the amplifiers by the laser mode-locking frequency. The amplified noise currents (i_1 and i_2) are then combined in a 0°/180° (\pm) combiner to give the sum ($i_+ = i_1 + i_2$) or difference ($i_- = i_1 - i_2$) noise current. The sum or difference noise current is fed by a RF SPDT switch into another amplifier and then fed into a spectrum analyzer for noise measurements. The balance of the homodyne detectors is carefully checked, and a typical common mode rejection of larger than 25 dB is observed for our measurement frequency range of 5–15 MHz. The difference current ($i_- = i_1 - i_2$) gives the shot-noise limit, and the sum current ($i_+ = i_1 + i_2$) gives the amplitude noise of the light field incident upon the homodyne detectors.

The Fano factor of the generated blue light is then measured by $F = \langle i_+^2 \rangle / \langle i_-^2 \rangle$, where $\langle i_+^2 \rangle$ represents the noise power of the sum current at a rf frequency and $\langle i_-^2 \rangle$ represents the noise power of the difference current (the shot-noise limit).⁷ The shot-noise level is typically ~ 6 dB higher than the dark-noise level at 8 MHz (with a resolution bandwidth of 300 kHz) for a dc current of 6 mA at each detector.^{7,12} The noise saturation was found for a dc

current of 10 mA at each detector, corresponding to ~ 40 -mW blue power incident upon each photodiode. The detector saturation effect at higher power has less effect on the measurements of the Fano factor in our detection scheme because both the sum current and the difference current have experienced the same saturation factor, and this factor is removed in their ratio.

4. RESULTS AND DISCUSSIONS

Figure 1 shows the total conversion efficiency of the SHG as the function of average input power, which we measured with a femtosecond (~ 120 -fs) pump and a picosecond (~ 2.0 -ps) pump, respectively. For these measurements, the crystal center was moved to near the focus position. For femtosecond input pulses, as shown in Fig. 1(a), the SHG conversion efficiency was found to increase as the average input power increases at the low input power but declines at much higher input powers. A maximum efficiency of $\sim 60\%$ was obtained at 110-mW input power. For picosecond input pulses, as shown in Fig. 1(b), similar efficiency ($\sim 56.5\%$) was observed at 100-mW input power. However, the conversion efficiency shows a damped oscillatory behavior at high input power: the conversion efficiency first declines after reaching its maximum and then recovers partially as the input power is increased before it decreases again. Such a difference between uses of picosecond and femtosecond pulses for SHG in a thick KNbO_3 crystal is quite significant. In femtosecond SHG, the decline in conversion efficiency with high input powers can be explained as the integrated effect of strong pump depletion over the whole crystal since pump depletion in each thickness l_T ($\sim 100 \mu\text{m}$) is very small and can be simply added together. However, in the

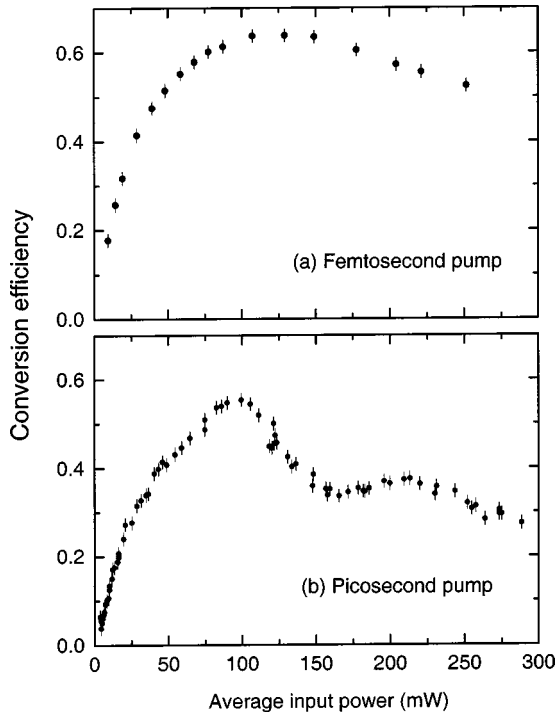


Fig. 1. Conversion efficiency of SHG in a KNbO_3 crystal as the function of average input power for (a) femtosecond pump (~ 120 fs), and (b) picosecond pump (~ 2.0 ps).

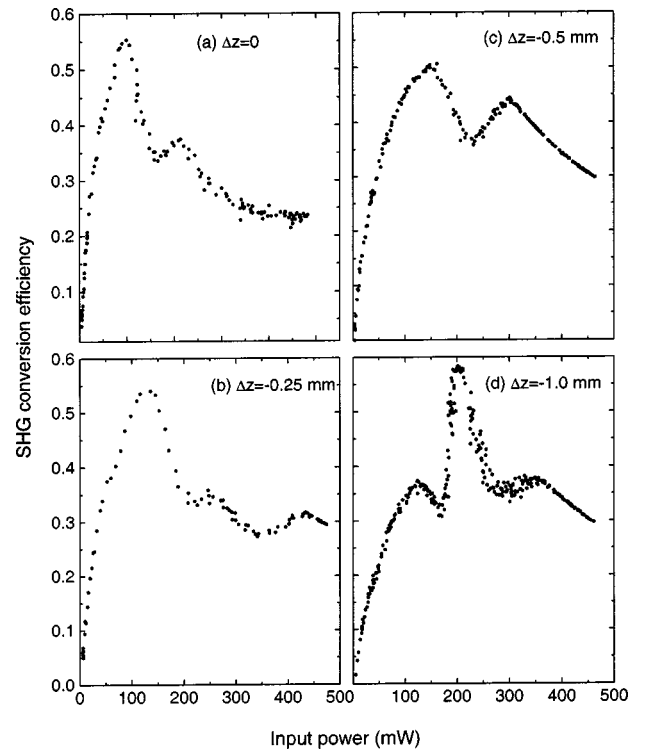


Fig. 2. Dependence of the conversion efficiency as a function of the input power for different values of the displacement between the center of the crystal and the beam focus of (a) $\Delta z = 0$, (b) $\Delta z = -0.25$ mm, (c) $\Delta z = -0.5$ mm, and (d) $\Delta z = -1.0$ mm. The input power at which the maximum efficiency is obtained is 100 mW, 125 mW, 150 mW, and 200 mW, respectively.

picosecond SHG, both the pump depletion and dephasing in the thickness l_T (~ 1.7 mm) are significantly larger. Obviously, the peak intensity of the picosecond input pulses is much lower (by a factor of ~ 20) than that of the femtosecond input pulses to reach the same optimum conversion efficiency.

The oscillatory decline of conversion efficiency in picosecond SHG in the strong focus condition can be understood as the combined effect of strong pump depletion and effective dephasing Δk_{eff} in the interaction length b .^{16–18} The effective dephasing Δk_{eff} includes contributions from mismatching Δk_0 between the fundamental and second-harmonic center wave vectors and from phase modulation of the fundamental pulse, which is given by $\Delta k_{\text{eff}} = \Delta k_0 + 2^{1/2}\phi_0/l_T$, where ϕ_0 is phase-modulation depth.¹⁶ The analytical solution for the SHG efficiency as a function of input intensity $I_\omega(0)$ is given by¹⁸

$$\frac{I_{2\omega}}{I_\omega} = \nu^2 s n^2 \left(\frac{\sqrt{\eta}}{\nu} \nu^4 \right), \quad (1)$$

with

$$\nu = [\Delta s/4 + \sqrt{1 + (\Delta s/4)^2}]^{-1}, \quad (2)$$

where sn is a Jacobian elliptic function, $\eta = kI_\omega(0)L^2$ is the nonlinear drive that is proportional to the input intensity of the fundamental field, and $\Delta s = \Delta k_{\text{eff}}L/\eta^{1/2}$. For strong focusing, the crystal length L is replaced by the depth of focus b . Conversion efficiency can be numeri-

cally calculated from Eq. (1), which shows an oscillatory decline as the input intensity increases for a nonzero dephasing Δk_{eff} .^{17,18}

The SHG conversion efficiency with picosecond pump pulses in a 10-mm-long NLC is very sensitive to the displacement Δz of the center of the crystal relative to the beam focal point along the beam-propagation direction. Figure 2 shows the measured conversion efficiencies as the function of the average input power for different values of the displacement. First, we moved the crystal with the translation stage such that the center of the crystal was near the position of the beam focal point, i.e., $\Delta z \approx 0$. As shown in Fig. 2(a), the maximum efficiency was obtained with an input power of ~ 100 mW. Then the crystal was moved toward the focal lens such that the beam focus was closer to the output surface of the crystal ($\Delta z < 0$). The maximum efficiency was obtained at a higher input power (~ 200 mW), and a “resonant” behavior was observed with $\Delta z = -1.0$ mm, as shown in Fig. 2(d). Figures 2(b) and 2(c) show the conversion efficiency for the other two focus positions ($\Delta z = -0.25$ mm and $\Delta z = -0.5$ mm, respectively). This position dependence of conversion efficiency for picosecond SHG is very different from that for femtosecond SHG in the strong focusing condition, in which the oscillatory decline of conversion efficiency was not observed.^{5,8}

Figure 3 shows the measured amplitude noise of the generated blue pulses with a homodyne detection setup for different values of the position displacement between the crystal center and the beam focus. The Fano factors in the figures are corrected for the generated blue light such that the dark noise is subtracted and the overall detection efficiency is corrected. Figure 3(a) shows the dependence of the Fano factor on input pump power at the

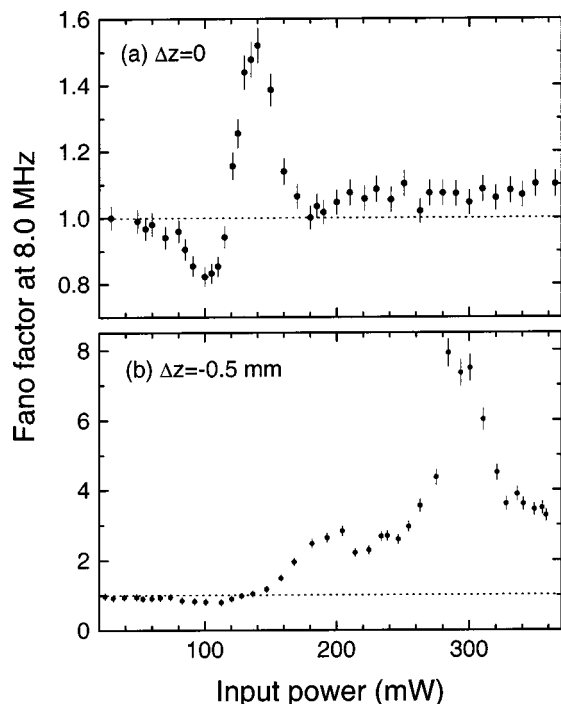


Fig. 3. Dependence of the measured Fano factor on the input power for (a) $\Delta z = 0$ and (b) $\Delta z = -0.5$ mm. Squeezing on the generated blue pulses was observed at low pump power.

frequency of 8.0 MHz (with a bandwidth of 300 kHz) for $\Delta z = 0$, and Fig. 3(b) shows the Fano factor for $\Delta z = -0.5$ mm. The correspondent conversion efficiencies are shown in Fig. 2(a) and Fig. 2(c), respectively. By comparing Fig. 3(a) to Fig. 2(a), one can see that, at low pump power, the conversion efficiency is low and the amplitude noise of the generated blue light is near the shot-noise limit. As the input pump power is increased, the conversion efficiency is increased and the amplitude noise is reduced below the shot-noise limit. The optimum measured Fano factor is $F = 0.82$ at the input power of 100 mW for $\Delta z = 0$ and $F = 0.79$ (21% squeezing) at 110 mW for $\Delta z = -0.5$ mm. However, as the input power is further increased, the dephasing and pump depletion effects become large, and the amplitude noise of the generated blue light is increased well above the shot-noise limit. The quantum noise of the blue pulses was sharply increased at a certain input power that is shifted with the focusing position. Complete understanding of the origin of such large quantum noises at large input powers and the factors that limit the amount of the observed squeezing with such high conversion efficiency in such a picosecond SHG system will require a full quantum-mechanical treatment of the system, including all nonlinear processes and loss mechanisms, which is beyond the scope of the current work.

5. CONCLUSION

In summary, we have measured the conversion efficiency and quantum-noise properties of the generated blue pulses in a highly efficient single-pass TW SHG with picosecond laser pulses and a thick KNbO_3 crystal. Under the strong focusing condition, both the conversion-efficiency and quantum-noise properties in the picosecond SHG are quite different from those in the femtosecond SHG. Although the conversion efficiency has reached $\sim 60\%$ for ~ 100 -mW input power, the peak intensity of the picosecond pulses is much lower than that of the femtosecond pulses (by a factor of ~ 20), which indicates that the picosecond SHG is more efficient in nonlinear interaction in such NLC. The conversion efficiency of the picosecond SHG declines oscillatorily as a function of input power, which shows the effective dephasing and strong pump-depletion effects under the condition of $l_T \sim b$, whereas the femtosecond SHG is similar to a quasi-phase-matching process under the condition of $l_T \ll b$. The quantum noise of the generated blue-light pulses was experimentally observed to be $\sim 20\%$ below the shot-noise limit, but the effective dephasing limits the degree of squeezing. The comparison between SHG with picosecond pulses and SHG with femtosecond pulses in this work may stimulate more theoretical interests in such systems, in which spectral width of the input field is comparable to the phase-matching width in the pulsed SHG. Also, such efficient SHG with low peak intensity could have practical applications in obtaining short-wavelength light beams.

ACKNOWLEDGMENTS

M. Xiao acknowledges the funding support from the National Science Foundation (PHY-9732431 and PHY-0099496) and the Office of Naval Research.

Yong-qing Li can be reached by telephone at 252-328-1858, or by e-mail at liy@mail.ecu.edu. Min Xiao can be reached by telephone at 479-575-6858, or by e-mail at mxiao@comp.uark.edu.

REFERENCES

1. P. Franken, A. Hill, C. Peters, and G. Weinreich, "Generation of optical harmonics," *Phys. Rev. Lett.* **7**, 118–119 (1961).
2. Y. A. Matveets, D. N. Nikogosyan, V. Kabelka, and A. Piskarskas, "Efficient second harmonic generation in a KDP crystal pumped with picosecond YAG:Nd³⁺ laser pulses of 0.5 Hz repetition frequency," *Sov. J. Quantum Electron.* **8**, 386–388 (1978).
3. W. Seka, S. D. Jacobs, J. E. Rizzo, R. Boni, and R. S. Craxton, "Demonstration of high efficiency third harmonic conversion of high power Nd-glass laser radiation," *Opt. Commun.* **34**, 469–473 (1980).
4. J. Reintjes and R. C. Eckardt, "Efficient harmonic generation from 532 to 226 nm in ADP and KD*P," *Appl. Phys. Lett.* **30**, 91–93 (1977).
5. A. M. Weiner, A. M. Kan'an, and D. E. Leaird, "High-efficiency blue generation by frequency doubling of femtosecond pulses in a thick nonlinear crystal," *Opt. Lett.* **23**, 1441–1443 (1998).
6. A. M. Kan'an and A. M. Weiner, "Efficient time-to-space conversion of femtosecond optical pulses," *J. Opt. Soc. Am. B* **15**, 1242–1245 (1998).
7. Y. Q. Li, D. Guzun, and M. Xiao, "Quantum-noise measurements in high-efficiency single-pass second-harmonic generation with femtosecond pulses," *Opt. Lett.* **24**, 987–989 (1999).
8. D. Guzun, Y. Q. Li, and M. Xiao, "Blue light generation in single-pass frequency doubling of femtosecond pulses in KNbO₃," *Opt. Commun.* **180**, 367–371 (2000).
9. D. K. Serland, P. Kumar, M. A. Arbore, and M. M. Fejer, "Amplitude squeezing by means of quasi-phase-matched second-harmonic generation in a lithium niobate waveguide," *Opt. Lett.* **22**, 1497–1499 (1997).
10. V. Pruneri, S. D. Butterworth, and D. C. Hanna, "Highly efficient green-light generation by quasi-phase-matched frequency doubling of picosecond pulses from an amplified mode-locked Nd:YLF laser," *Opt. Lett.* **21**, 390–392 (1996).
11. S. Youn, S.-K. Choi, P. Kumar, and R.-D. Li, "Observation of sub-Poissonian light in traveling-wave second-harmonic generation," *Opt. Lett.* **21**, 1597–1599 (1996).
12. Y. Q. Li, D. Guzun, and M. Xiao, "Sub-shot-noise-limited optical heterodyne detection using an amplitude-squeezed local oscillator," *Phys. Rev. Lett.* **82**, 5225–5228 (1999).
13. E. S. Polzik and H. J. Kimble, "Frequency doubling with KNbO₃ in an external cavity," *Opt. Lett.* **16**, 1400–1402 (1991).
14. P. Lodahl, J. L. Sorensen, and E. S. Polzik, "High efficiency second harmonic generation with a low power diode laser," *Appl. Phys. B* **64**, 383–386 (1997).
15. H. Tsuchida, "Generation of amplitude-squeezed light at 431 nm from a singly resonant frequency doubler," *Opt. Lett.* **20**, 2240–2242 (1995).
16. R. C. Eckardt, "Phase matching limitations of high efficiency second harmonic generation," *IEEE J. Quantum Electron.* **QE-20**, 1178–1187 (1984).
17. D. Eimerl, "High average power harmonic generation," *IEEE J. Quantum Electron.* **QE-23**, 575–592 (1987).
18. D. Perlov and M. Roth, "Efficiency of non-phase-matched second harmonic generation by Gaussian pulses," *Appl. Opt.* **36**, 5010–5017 (1997).